Available online at www.sciencedirect.com
SCIENCE DIRECT®
Nuclear Instruments and Methods in Physics Research A 560 (2006) 309–316
NUCLEAR INSTRUMENTS & METHODS IN PHYSICS RESEARCH Section A
www.elsevier.com/locate/nima

16-point discrete Fourier transform based on the Radix-2 FFT algorithm implemented into cyclone FPGA as the UHECR trigger for horizontal air showers in the Pierre Auger Observatory

Z. Szadkowski*,[1]

Physics Department, Bergische Universität Wuppertal, 42097 Wuppertal, Germany

Received 19 October 2005; accepted 10 January 2006
Available online 10 February 2006

Abstract

Extremely rare flux of UHERC requires sophisticated detection techniques. Standard methods oriented on the typical events may not be sensitive enough to capture rare events, crucial to fix a discrepancy in the current data or to confirm/reject some new hypothesis. Currently used triggers in water Cherenkov tanks in the Pierre Auger surface detector, which select events above some amplitude thresholds or investigate a length of traces are not optimized to the horizontal and very inclined showers, interesting as potentially generated by neutrinos. Those showers could be triggered using their signatures: i.e. a curvature of the shower front, transformed on the rise time of traces or muon component giving early peak for "old" showers. Currently available powerful and cost-effective FPGAs provide sufficient resources to implement new triggers not available in the past. The paper describes the implementation proposal of 16-point discrete Fourier transform based on the Radix-2 FFT algorithm into Altera Cyclone FPGA, used in the 3rd generation of the surface detector trigger. All complex coefficients are calculated online in heavy pipelined routines. The register performance ~200 MHz and relatively low resources occupancy ~2000 logic elements/channel for 10-bit resolution provide a powerful tool to trigger the events on the traces characteristic in the frequency domain. The FFT code has been successively merged to the code of the 1st surface selector level trigger of the Pierre Auger Observatory and is planned to be tested in real pampas environment.

PACS: 29.40; 85.40; 95.30.−k

Keywords: FFT; FPGA; Pierre Auger Observatory; Triggers

1. Introduction

Extensive Air Showers are investigated in several experiments utilizing different detection techniques (scintillators, water Cherenkov and fluorescence detectors). Signals in the detectors depend on several parameters such as the energy, the type of the primary particle, distance from the core, the angle of registered shower, etc.

Usually the triggering conditions are chosen such as to detect as wide as possible classes of events. However, sometimes the standard trigger conditions are not optimized for the specific class of events, which are either not registered at all or for which the registration efficiency is poor.

In experiments utilizing water Cherenkov detectors, signals from photo-multipliers are usually digitized in Flash ADCs and next processed by often-sophisticated electronics. In order to increase the signal/noise ratio coincidence techniques are widely used. Typically signals from PMTs are analyzed online in both amplitude and time domains. Strong signals in all PMT channels, corresponding to energetic showers detected near the core, are

*Tel.: +49 202 439 3736; fax: +49 202 439 2662.
E-mail address: zszadkow@physik.uni-wuppertal.de.
[1]On leave from University of Łódź, Pomorska 151, 90-236 Łódź, Poland.

0168-9002/$ - see front matter © 2006 Elsevier B.V. All rights reserved.
doi:10.1016/j.nima.2006.01.045

registered because of many-fold coincidence single bin trigger with a fixed thresholds. Showers detected far from the core give much lower signals usually spread in time. Such events are detected by the other type of trigger investigating the structure of signal in some period (in a sliding time window).

Both types of triggers do not seem to be optimized for very inclined or horizontal showers, also generated by neutrinos. The signals from that type of showers are usually too low to be detected by the single bin trigger. On the other hand, the signals could be too short to provide sufficient occupancy to be detected by a Time over Threshold trigger (ToT) [1].

2. Deep showers

The structure of signals detected in water Cherenkov tanks and generated by horizontal showers depend strongly on the point of the EAS initialization. "Old" showers (see Fig. 1) generated by hadrons early in the atmosphere give flat muonic front; showers generated by deeply interacting neutrinos are characterized by a curved front (radius of curvature of a few km), a large electromagnetic component and with particles spread over a few microseconds interval [2]. In both cases muonic front produces a bump, which can be a starting signature of horizontal showers. The bump for the "old" showers is shorter and sharper than for the "young" ones and results in a larger contribution in higher Fourier coefficients. For "young" showers, with relatively smooth shape of a signal profile, the lower Fourier components should dominate. The online analysis of the Fourier components may trigger specific events.

The existing software procedures, available as commercial IP routines, can calculate Fourier coefficients effectively utilizing a FFT algorithm. However the software implementation is too slow to be able to trigger events in the real time. Online triggering requires the hardware implementation calculating multipoint DFT with a sufficient speed. Modern powerful FPGAs can do this job, however, the resource requirement increases dramatically with the number of points. The analysis time interval should be a reasonable compromise between a time resolution and the resources occupancy in the FPGA.

3. General algorithm

Let us consider a DFT $\bar{X}$ of dimension N [3]

$$\bar{X}_k = \sum_{m=0}^{N-1} x_m W^{mk} \tag{1}$$

where $W = e^{-j2\pi/N}$ and $k = 0, \ldots, N-1$.

If N is the product of two factors, with $N = N_1 N_2$, the indices m and k we can redefined as follows: $m = N_1 m_2 + m_1$,

where $m_2 = 0, \ldots, N_2 - 1$ and $m_1 = 0, \ldots, N_1 - 1$,

$k = N_2 k_1 + k_2$, $k_2 = 0, \ldots, N_2 - 1$

and $k_1 = 0, \ldots, N_1 - 1$

$$\bar{X}_{N_2 k_1 + k_2} = \sum_{m_1=0}^{N_1-1} W^{N_2 m_1 k_1} W^{m_1 k_2} \times \sum_{m_2=0}^{N_2-1} x_{N_1 m_2 + m_1} W^{N_1 m_2 k_2}. \tag{2}$$

For the Radix-2 algorithm: $N = 2^t$, $N_1 = 2$ and $N_2 = 2^{t-1} = N/2$. Hence,

$$\bar{X}_k = \sum_{m=0}^{N/2-1} (x_{2m} + W^k x_{2m+1}) W^{2mk}. \tag{3}$$

If we split the sum as follows

$$\bar{X}_k = \sum_{m=0}^{N/4-1} x_{2m} W^{2mk} + \sum_{m=N/4}^{N/2-1} x_{2m} W^{2mk} + \sum_{m=0}^{N/4-1} x_{2m+1} W^{2mk} + \sum_{m=N/4}^{N/2-1} x_{2m+1} W^{2mk} \tag{4}$$

and afterwards, if we redefine indices and group the sums, we get,

$$\bar{X}_k = \sum_{m=0}^{N/4-1} (x_{2m} + (-1)^k x_{2(m+N/4)}) W^{2mk} + W^k \left(\sum_{m=0}^{N/4-1} (x_{2m+1} + (-1)^k x_{2(m+N/4)+1} \right) W^{2mk}. \tag{5}$$

We can introduce the new set of variables defined for $m = 0, \ldots, N/4 - 1$ as follows:

$$A_{2m} = x_{2m} + x_{2m+N/2} \tag{6}$$

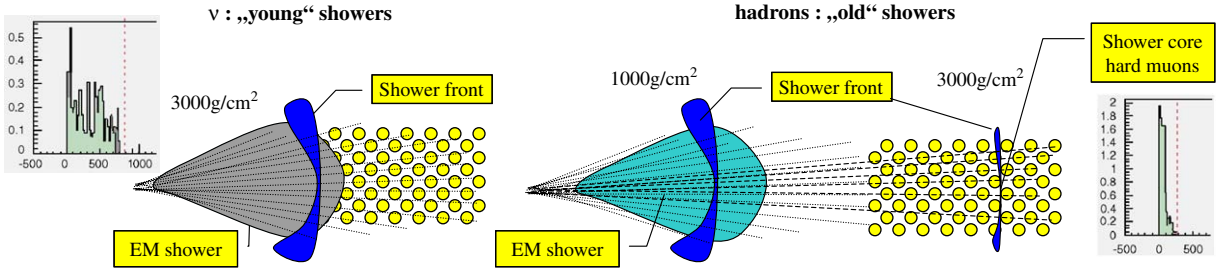

Fig. 1. Development of showers generated deeply and early in the atmosphere.

$$A_{2m+1} = x_{2m+1} + x_{2m+1+N/2} \tag{7}$$

$$A_{2m+N/2} = x_{2m} - x_{2m+N/2} \tag{8}$$

$$A_{2m+1+N/2} = x_{2m+1} - x_{2m+1+N/2}. \tag{9}$$

We get

$$\bar{X_k} = \sum_{m=0}^{N/4-1} (A_{2m} + W^k A_{2m+1}) W^{2mk} \tag{10}$$

$$\bar{X_k} = \sum_{m=0}^{N/4-1} (A_{2m+N/2} + W^k A_{2m+1+N/2}) W^{2mk} \tag{11}$$

for k even and odd, respectively.

x_m represent signals in time domain. They can be easily available from outputs of shift registers clocked synchronously with FADC.

The DFT coefficients $\bar{X_k}$ can be expressed by new set of variables A_m, Because A_m are simple linear combination of x_m, they can be calculated by typical adders (Eqs. (6) and (7)) and sub-tractors (Eqs. (8) and (9)) in a single clock cycle. The input values x_m are real and positive, since they represent the signal in the real time.

Coefficients of DFT in the real domain additional simplify due to the following symmetry:

$$\mathrm{Re}(\bar{X_k}) = +\mathrm{Re}(\bar{X}_{N-k}), \tag{12}$$

$$\mathrm{Im}(\bar{X_k}) = -\mathrm{Im}(\bar{X}_{N-k}). \tag{13}$$

The Radix-2 algorithm allows on regrouping of inputs elements in the DFT expression in order to utilize some symmetries of Fourier coefficients. In a single step of the Radix-2 algorithm we can redefine the "new" set of variables by some mathematical expression of the "old" ones. This step will correspond to an elementary process in the pipeline chain. The redefinition of variables in Eqs. (6)–(9) corresponds to the 1st stage of the pipeline. Splitting the sum (3) reduces of coefficient W^k set from $0,\ldots,N-1$ for input x_m to $0,\ldots,(N/2)-1$ for Eqs. (10) and (11). The 1st stage utilizes the feature of the twiddle factors related to the 1st stage of the pipeline.

$$W_A = W^{N/2} = \mathrm{e}^{-\mathrm{j}\pi} = -1. \tag{14}$$

So, the 1st stage can be implemented in a very simple way. The implementation of the multi-points algorithm requires multiple pipeline stages and apart from adders and sub-tractors also requires multipliers, which correspond to the W^k coefficients relating to the fractional "angle" $\mathrm{e}^{-\mathrm{j}2k\pi/N}$. The Radix-2 algorithm used in the next stage reduces again the abundance of W^k coefficients due to the next twiddle factors' related to the 2nd stage of the pipeline.

$$W_B = W^{N/4} = \mathrm{e}^{-\mathrm{j}\pi/2} = -\mathrm{j}. \tag{15}$$

The W_B suggests the similar splitting structure in the 2nd pipeline stage as in the 1st one (minus in Eq. (15) as in Eq. (14)), however, the imaginary unit imposes the DFT calculation separately for their real and imaginary parts.

If we split the sum in (11) similar as in (4), we get for $k = 0, 2, \ldots, N-2$

$$\bar{X}_k = \sum_{m=0}^{N/8-1} \left[(A_{2m} + (-\mathrm{j})^k A_{2m+N/4}) W^{2mk} + (A_{2m+1} + (-\mathrm{j})^k A_{2m+1+N/4}) W^{(2m+1)k}\right]. \tag{16}$$

Let us consider separately two subset of odd indices: $k = 4n$ and $k = 4n+2$ $(n = 0,\ldots,N/4-1)$

$$\bar{X}_{4n} = \sum_{m=0}^{N/8-1} \left[(A_{2m} + A_{2m+N/4}) W^{8mn} + (A_{2m+1} + A_{2m+1+N/4}) W^{(2m+1)4n}\right]. \tag{17}$$

Notice that $\bar{X}_0$ and $\bar{X}_{N/2}$ are real.

$$\bar{X}_{4n+2} = \sum_{m=0}^{N/8-1} \left[(A_{2m} - A_{2m+N/4}) W^{8m(4n+2)} + (A_{2m+1} - A_{2m+1+N/4}) W^{(2m+1)(4n+2)}\right]. \tag{18}$$

If we introduce new variables

$$B_{2m} = A_{2m} + A_{2m+N/4} \tag{19}$$

$$B_{2m+1} = A_{2m+1} + A_{2m+1+N/4} \tag{20}$$

$$B_{2m+N/2} = A_{2m} - A_{2m+N/4} \tag{21}$$

$$B_{2m+1+N/2} = A_{2m+1} - A_{2m+1+N/4}. \tag{22}$$

We get

$$\bar{X}_{4n} = \sum_{m=0}^{N/8-1} (B_{2m} + B_{2m+1} W^{4n}) W^{8mn}, \tag{23}$$

$$\bar{X}_{4n+2} = \sum_{m=0}^{N/8-1} (B_{2m+N/4} + B_{2m+1+N/4} W^{4n+2}) W^{8mn+4m}. \tag{24}$$

However, repeating the above procedure for odd indices related to Eq. (11) gives more complicated formulae, which cannot be simplified due to complex coefficients $W^{4(n+p)}$ (Eq. (25)).

$$\bar{X}_{4n+p} = \sum_{m=0}^{N/8-1} W^{2m(4n+p)} \times \left[(A_{2m+N/2} + A_{2m+1+N/2} W^{4(n+p)}) \mp \mathrm{j}(A_{2m+3N/4} + A_{2m+1+3N/4} W^{4(n+p)})\right] \tag{25}$$

where $\mp$ corresponds to $p = 1, 3$, respectively.

Next simplification is possible due to symmetries of trigonometric functions. However, general considerations give relatively complicated formulae, which seem to be unnecessary here.

4. Timing

The algorithm described here is planned to be experimentally verified on the Auger South array. Therefore, the FPGA chip must be selected as in the 1st level Auger trigger [4]. Preliminary analysis of resources occupancy in the Cyclone EP1C12Q240I7 chip suggests a limitation to the DFT points $N = 16$. A 16-point structure clocked with 40 MHz gives the DFT in 400 ns window. This interval seems to be sufficient for the preliminary analysis of the muonic bump, especially for the "old" showers. Nevertheless, "young" showers can be treated as pre-trigger, turning on the channel investigating next the signal over longer microsecond time, corresponding to the electromagnetic component of the shower. The enlarged length of shift registers (by the factor 16) can provide an analysis in 6.4 μs sliding window. If the pre-trigger appears, the same hardware FFT structure is multiplexed to the boxcar integration circuit, integrating data over 16 time bins (see Fig. 5 in Ref. [5]).

5. 16-point algorithm

For $N = 16$ and odd indices we get,

$$\begin{aligned}\bar{X}_{4n+p} = {} & (A_8 \mp \mathrm{j}A_{12}) \\ & + (\mathrm{j})^n(A_9(-1)^n W^p - \mathrm{j}A_{15}W^{4-p}) \\ & + (-\mathrm{j})^{(p-1)/2}(-1)^n W^2(A_{10} \mp \mathrm{j}A_{14}) \\ & \pm (\mathrm{j})^n(A_{11}W^{4-p} - \mathrm{j}A_{13}(-1)^n W^p). \end{aligned} \tag{26}$$

Since of $W^4 = -\mathrm{j}$, all coefficients can be expressed as a linear combination of the complex base W^1, W^2, W^3

$$W^1 = \cos\left(\frac{\pi}{8}\right) - \mathrm{j}\,\sin\left(\frac{\pi}{8}\right) = \alpha - \mathrm{j}\beta \tag{27}$$

$$W^2 = \cos\left(\frac{\pi}{4}\right) - \mathrm{j}\,\sin\left(\frac{\pi}{4}\right) = \gamma(1 - \mathrm{j}) \tag{28}$$

$$W^3 = \cos\left(\frac{3\pi}{8}\right) - \mathrm{j}\,\sin\left(\frac{3\pi}{8}\right) = \beta - \mathrm{j}\alpha. \tag{29}$$

Some symmetry in Eqs. (27)–(29) allows the following simplification. Notice that

$$W^2(A_{10} \mp \mathrm{j}A_{14}) = \gamma[(A_{10} \mp A_{14}) \mp \mathrm{j}(A_{10} \mp A_{14})] \tag{30}$$

$$\begin{aligned} & A_9(-1)^n W^p - \mathrm{j}A_{15}W^{4-p} \\ & \quad = \widehat{\mathscr{X}}[(-1)^n(A_9 - A_{15})] - \mathrm{j}\widehat{\mathscr{Y}}[(-1)^n(A_9 + A_{15})] \end{aligned} \tag{31}$$

$$\begin{aligned} & A_{11}W^p - \mathrm{j}A_{13}(-1)^n W^{4-p} \\ & \quad = \widehat{\mathscr{Y}}[A_{11} - (-1)^n A_{13})] - \mathrm{j}\widehat{\mathscr{X}}[A_{11} + (-1)^n A_{13})] \end{aligned} \tag{32}$$

where $\widehat{\mathscr{X}} = \alpha, \beta, \widehat{\mathscr{Y}} = \beta, \alpha$ for $p = 1, 3$

We can extend the set of variable Eqs. (19)–(22) also to odd indices of $\bar{X}$

$$B_8 = A_8, \quad B_{12} = A_{12} \tag{33}$$

$$B_9 = A_9 + A_{15}, \quad B_{15} = A_9 - A_{15} \tag{34}$$

$$B_{10} = A_{10} + A_{14}, \quad B_{14} = A_{10} - A_{14} \tag{35}$$

$$B_{11} = A_{11} + A_{13}, \quad B_{13} = A_{11} - A_{13}. \tag{36}$$

Formulae (33)–(36) show that the entire 2nd pipeline stage can be built also from only adders and sub-tractors. Signals (33) have to be delayed in parallel shift registers in order to assure synchronization with adjacent ones.

For $N = 16$ the DFT coefficients can be expressed by the B_m variables as follows

$$\mathrm{Re}(\bar{X}_0) = B_0 + B_1 + B_2 + B_3 \tag{37}$$

$$\mathrm{Re}(\bar{X}_8) = B_0 - B_1 + B_2 - B_3 \tag{38}$$

$$\mathrm{Re}(\bar{X}_4) = B_0 - B_2 \tag{39}$$

$$\mathrm{Re}(\bar{X}_2) = B_4 + \gamma(B_5 - B_7) \tag{40}$$

$$\mathrm{Re}(\bar{X}_6) = B_4 - \gamma(B_5 - B_7) \tag{41}$$

$$\mathrm{Im}(\bar{X}_2) = -B_6 - \gamma(B_5 + B_7) \tag{42}$$

$$\mathrm{Im}(\bar{X}_6) = B_6 - \gamma(B_5 + B_7) \tag{43}$$

$$\mathrm{Re}(\bar{X}_{1,7}) = B_8 \pm \alpha B_{15} + \gamma B_{14} \pm \beta B_{13} \tag{44}$$

$$\mathrm{Re}(\bar{X}_{3,5}) = B_8 \pm \beta B_{15} - \gamma B_{14} \mp \alpha B_{13} \tag{45}$$

$$\mathrm{Im}(\bar{X}_{1,7}) = \mp B_{12} - \beta B_9 \mp \gamma B_{10} - \alpha B_{11} \tag{46}$$

$$\mathrm{Im}(\bar{X}_{3,5}) = \pm B_{12} - \alpha B_9 \mp \gamma B_{10} + \beta B_{11}. \tag{47}$$

The next, 3rd pipeline stage requires implementation of 10 multipliers calculating products from (44–47), 3 adders, 3 sub-tractors and 4 shift registers. according to the following formulae

$$C_0 = B_0 + B_2, \quad C_{9A} = \alpha B_9 \tag{48}$$

$$C_1 = B_1 + B_3, \quad C_{9B} = \beta B_9 \tag{49}$$

$$C_2 = B_0 - B_2, \quad C_{10} = \gamma B_{10} \tag{50}$$

$$C_3 = B_1 - B_3, \quad C_{11A} = \alpha B_{11} \tag{51}$$

$$C_5 = B_5 + B_7, \quad C_{11B} = \beta B_{11} \tag{52}$$

$$C_7 = B_5 - B_7, \quad C_{13A} = \alpha B_{13} \tag{53}$$

$$C_4 = B_4, \quad C_{13B} = \beta B_{13} \tag{54}$$

$$C_6 = B_6, \quad C_{14} = \gamma B_{14} \tag{55}$$

$$C_8 = B_8, \quad C_{15A} = \alpha B_{15} \tag{56}$$

$$C_{12} = B_{12}, \quad C_{15B} = \beta B_{15}. \tag{57}$$

The 4th stage utilizes 2 multipliers, 5 adders, 5 subtractors and 4 shift registers

$$D_5 = \gamma C_5, \quad D_7 = \gamma C_7 \tag{58}$$

$$D_0 = C_0 + C_1, \quad D_1 = C_0 - C_1 \tag{59}$$

$$D_8 = C_8 + C_{14}, \quad D_9 = C_{9A} - C_{11B} \tag{60}$$

$$D_{10} = C_{10} + C_{12}, \quad D_{12} = C_{10} - C_{12} \tag{61}$$

$$D_{11} = C_{11A} + C_{9B}, \quad D_{15} = C_{13A} - C_{15B} \tag{62}$$

$$D_{13} = C_{13B} + C_{15A}, \quad D_{14} = C_8 - C_{14} \tag{63}$$

$$D_2 = C_2, \quad D_3 = C_3 \tag{64}$$

$$D_4 = C_4, \quad D_6 = C_6. \tag{65}$$

Finally in the 5th stage the set of DFT $\bar{X}_k$ coefficients is calculated by 6 adders and 6 sub-tractors supported by 4 shift registers.

$$\mathrm{Re}\,\bar{X}_0 = D_0, \quad \mathrm{Re}\,\bar{X}_1 = D_8 + D_{15} \tag{66}$$

$$\mathrm{Re}\,\bar{X}_2 = D_4 + D_7, \quad \mathrm{Re}\,\bar{X}_3 = D_{14} - D_{13} \tag{67}$$

$$\mathrm{Re}\,\bar{X}_4 = D_2, \quad \mathrm{Re}\,\bar{X}_5 = D_{14} + D_{13} \tag{68}$$

$$\mathrm{Re}\,\bar{X}_6 = D_4 - D_7, \quad \mathrm{Re}\,\bar{X}_7 = D_8 - D_{15} \tag{69}$$

$$\mathrm{Re}\,\bar{X}_8 = D_1, \tag{70}$$

$$\mathrm{Im}\,\bar{X}_1 = -(D_{10} + D_{11}) \tag{71}$$

$$\mathrm{Im}\,\bar{X}_4 = -D_3, \quad \mathrm{Im}\,\bar{X}_2 = -(D_6 + D_5) \tag{72}$$

$$\mathrm{Im}\,\bar{X}_6 = D_6 - D_5, \quad \mathrm{Im}\,\bar{X}_3 = -(D_{12} + D_9) \tag{73}$$

$$\mathrm{Im}\,\bar{X}_7 = D_{10} - D_{11}, \quad \mathrm{Im}\,\bar{X}_5 = D_{12} - D_9. \tag{74}$$

6. FPGA implementation

The structure of the routines implemented into FPGA is presented on the Fig. 2. Two first two pipeline stages utilize adders and differential circuits only, and can be implemented as the single bin routines; however, multipliers need at least two clock cycles to assure a sufficient registered performance. Some signals (i.e. $B_8 = A_8$), which do not require any mathematical calculation, have to be delayed in

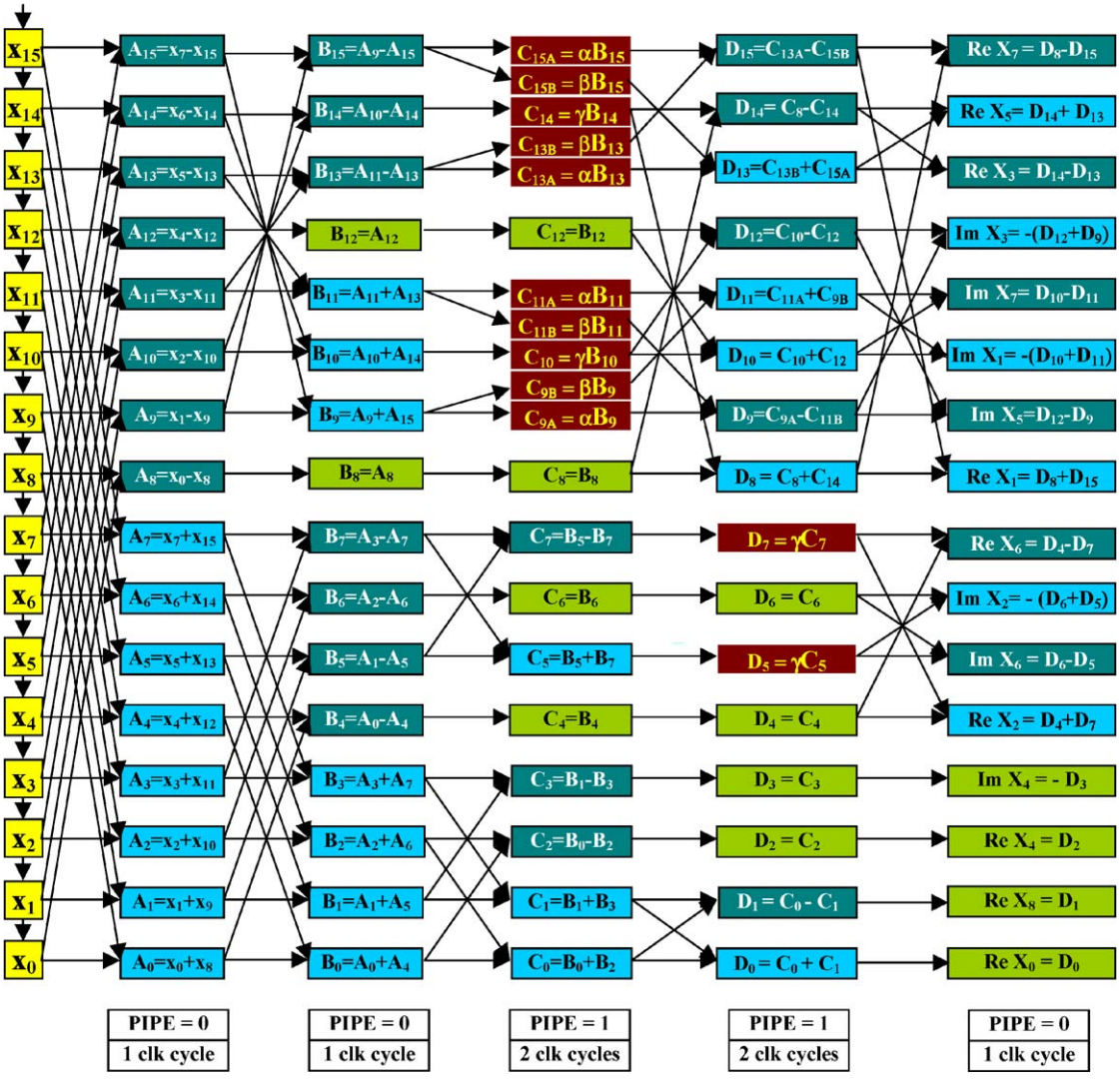

Fig. 2. Global pipeline internal structure of FFT.

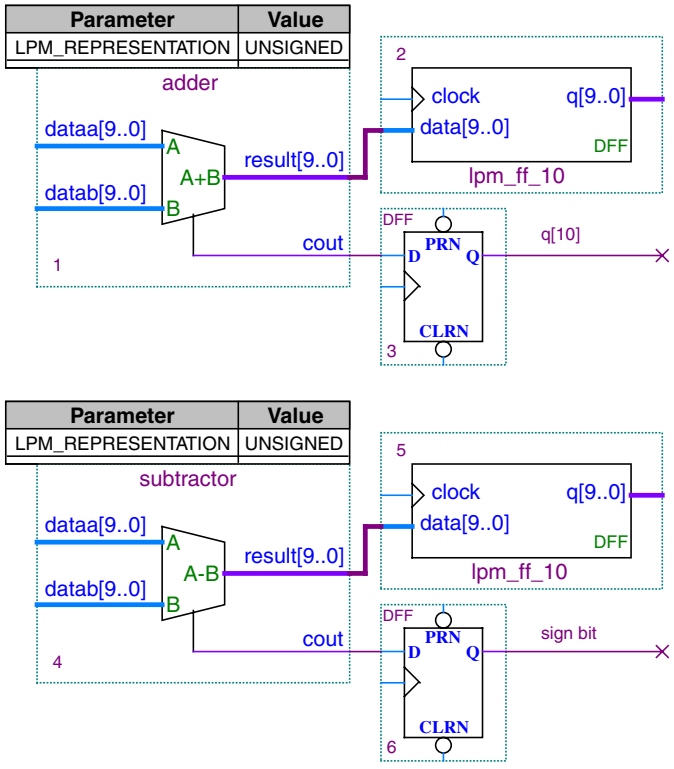

Fig. 3. Adders and sub-tractors in the 1st pipeline stage. For adders count is the 10th bit of the value, for sub-tractors is the sign bit. Both adders and sub-tractors are implemented as "unsigned" LPM (inputs from shift registers are always positive).

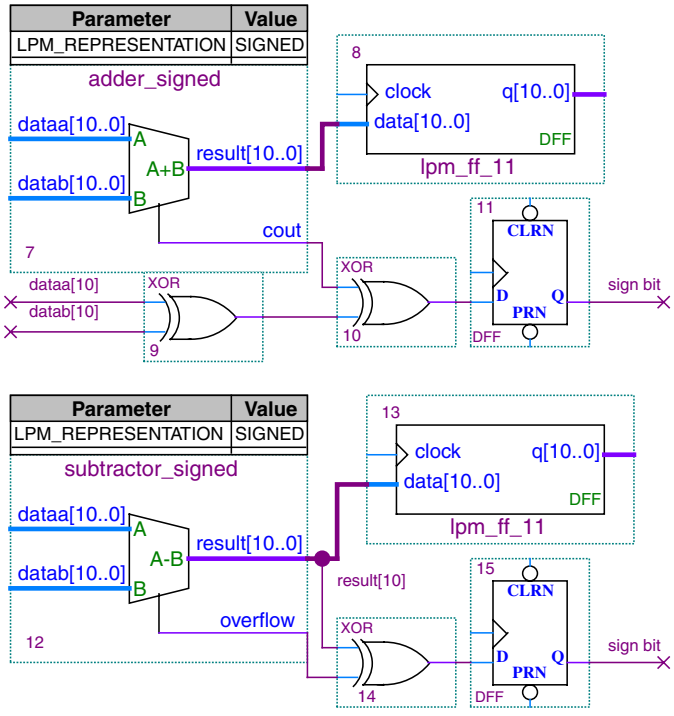

Fig. 4. Adders and sub-tractors in the 2nd pipeline stage. dataa [10] and datab [10] are the sign bits.

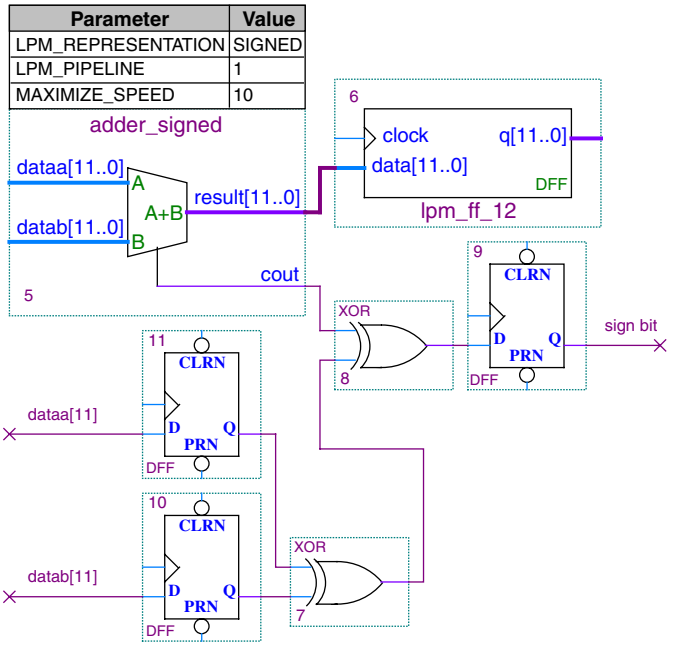

Fig. 5. Adders in the 3rd pipeline stage. The input sign bits dataa [11] and datab [11] have to be delayed on the single clock cycle, due to pipelined implementation.

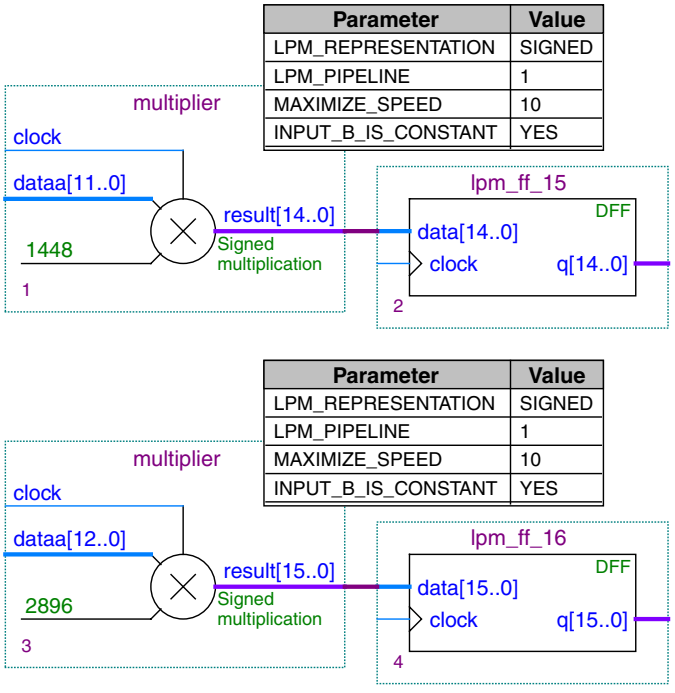

Fig. 6. Pipelined multiplier in the 3rd stage (above). Input integer dataa is multiplied by the constant fractional coefficient implemented here as the fixed point value. 12-bit signed representation of the γ coefficient gives the value 1448 (1892 and 782 for α and β, respectively). Multiplication of two 12-bit factors gives as result 24-bit value. However, the result from multiplier is shrinked to 15 bits only (in order to save resources), which gives additional 3 bits of better accuracy (in comparison with the pure shrink of the input 12-bit signed data by the scaling γ factor). In the 4th stage (below) 13-bit signed representation of the γ coefficient gives the value 2896. The result from multiplier is shrinked to 16 bits only.

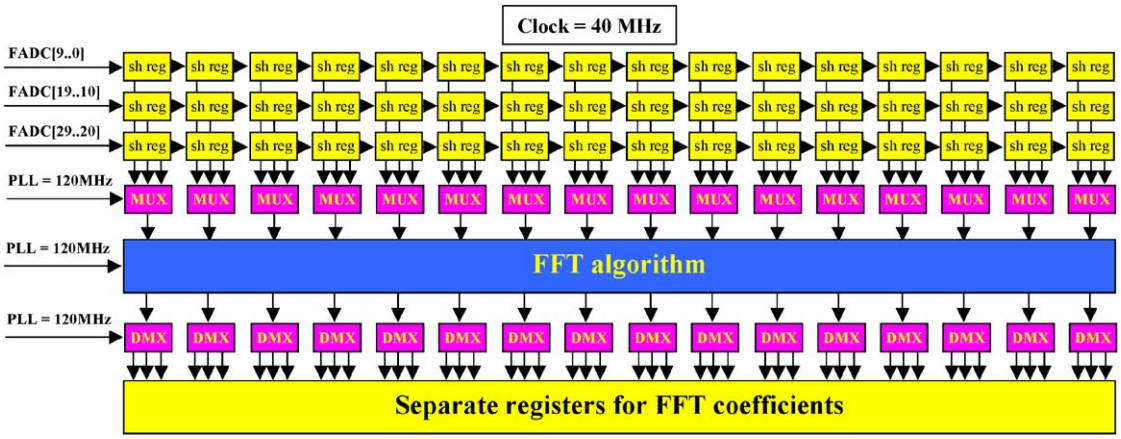

Fig. 7. The mux-demux structure allowing a calculation of FFT coefficients independently for three channels with triple PLL clock.

appropriate registers in order to assure the correct synchronization.

The algorithm has been implemented for a 10-bit FADC bus into the Cyclone EP1C12Q240I7 Altera chip, with 40 MHz clock (as in the first level surface detector trigger in the Pierre Auger Observatory [5–7]). It requires 12 multipliers, 28 adders, 29 differential circuits and 12 delaying routines (simple registers) for synchronization—totally ~2000 logic elements. Fixed point multiplication provides an accuracy on the level 0.05% (multiplication of two 12-bit factors gives as result 24-bit value, however, the result from multiplier is shortened to 15 bits only (in order to save resources), which provides an additional 3 bits of accuracy (in comparison with the pure cut-off of the input 12-bit signed data by the scaling factor).

In order to minimize the resource occupancy the AHDL code utilizes the Library of Parameterized Modules (LPM) with "unsigned" parameters, where possible and the fixed point multiplication structure, where the size of the fractional part is arbitrarily fixed. The intermediate results of multiplications are approximated on the next pipeline stage after next sum/difference. Re and Im coefficients are finally calculated with 10-bit resolution.

More useful than pure real and imaginary coefficients seems to be "coefficients of the power spectrum density": $\{\xi = \mathrm{Re}\,\bar{X}_k\}^2 + \{\mathrm{Im}\,\bar{X}_k\}^2$ which can be calculated by the "square devices" (see Figs. 3–7 in Ref. [5]).

7. Integration with the Auger code

The Auger surface detector contains 1600 cylindrical water Cherenkov tanks arranged on a hexagonal grid. The Cherenkov light produced by the electromagnetic component of EAS is detected by three PMTs. The PMT signals from the last dynode (high-gain channel) and anode (low-gain channel) are continuously digitized at 40 MHz by six 10-bit FADCs [1], providing 15-bit dynamic range. However, the trigger is generated from the high-gain channel only (from three 10-bit channels).

The design of the Auger surface detector trigger has been continually optimized and improved, due to the progress in electronics. The 1st and 2nd generations of triggers, based on APEX [6] and ACEX [7] Altera® PLD families, respectively, contained relatively limited resources and did not allow an implementation more sophisticated algorithms. The newest 3rd generation based on Cyclone Altera® FPGA [4,5,8] and containing much more resources than the previous designs, allow integration the FFT algorithm together with the main Auger trigger code. Deployment of this 3rd generation began in November 2005.

The very high registered performance of the FFT routine ($\geqslant$200 MHz) allows a utilization of the same logical structure for three 10-bit FADC channels multiplexing with three times the frequency of the global clock (generated internally by PLL)).

The FFT code has been successively merged with the Auger code. The Auger input data from three shift registers (corresponding to three high-gain channels) are multiplexed with 120 MHz and are fed into the FFT routine as a whole. The output FFT coefficients, calculated inside the FFT routine, are next de-multiplexed and stored in separate registers. They are then available for each channel independently and can be used for a trigger with the standard clock = 40 MHz. The initial resources occupancy increased from 54% to 78%. The final registered performance of the global code is on the level 140 MHz, which gives a sufficient safety margin [9].

The 3rd generation of the surface detector trigger is planned to be deployed in the 2nd half of the Auger Southern array.

8. Conclusions

The 16-point implementation of the FFT into an FPGA seems to be a powerful tool for the spectral analysis of the FADC traces. The results presented above focus rather on the hardware FPGA implementation, precise conditions for triggering are still subjected to simulation and

optimization of relations between different Fourier coefficients or power spectral densities. The 32-point algorithm required many more multipliers and adders, and can be implemented much more effectively in chips with hard-core DSP blocks like i.e. Altera® Stratix™ or Cyclone II.

900 Cherenkov tanks on the Auger Southern array are equipped with the 2nd generation design, the next 700 will be equipped with the 3rd generation one. Due to the required homogeneity, the official code must be the same on the entire array. Nevertheless, the 2nd half of the Auger South is capable of investigating non-standard algorithms, which finally can be used either on limited array section or in the Auger North.

Acknowledgements

This work was funded by the Polish Committee of Science under grant No. 1 PO3D 01430.

References

[1] Pierre Auger Collaboration, Nucl. Instr. and Meth. A 523 (2004) 50.
[2] X. Bertou, P. Billoir, O. Deligny, C. Lachaud, A. Letessier-Selvon, astro-ph/ 0104452.
[3] H.J. Nussbauer, Fast Fourier Transform and Convolution Algorithms, Springer, Berlin, 1981.
[4] Z. Szadkowski, A proposal of a Single Chip Surface Detector Trigger based on Altera® Cyclone™ Family, in: Proceedings of the 28th ICRC, Tsukuba, 2003.
[5] Z. Szadkowski, K.-H. Becker, K.-H. Kampert, Nucl. Instr. and Meth. A 545 (2005) 793.
[6] Z. Szadkowski, D. Nitz, Nucl. Instr. and Meth. A 545 (2005) 624.
[7] Z. Szadkowski, Nucl. Instr. and Meth. A 551 (2005) 477.
[8] Z. Szadkowski, K.-H. Becker, K.-H. Kampert, 3rd Generation of the First Level Trigger for the Surface Array in the Pierre Auger Observatory based on the Cyclone™ Altera® FPGA, in: Proceedings of the 29th ICRC, Pune, 2005.
[9] Z. Szadkowski, 16-point Discrete Fourier transform based on the Radix-2 FFT algorithm implemented into Cyclone FPGA as the UHERC trigger for horizontal air showers, in: Proceedings of the 29th ICRC, Pune, 2005.